

TAVGBench: Benchmarking Text to Audible-Video Generation

Anonymous Authors

ABSTRACT

The Text to Audible-Video Generation (TAVG) task involves generating videos with accompanying audio based on text descriptions. Achieving this requires skillful alignment of both audio and video elements. To support research in this field, we have developed a comprehensive Text to Audible-Video Generation Benchmark (TAVGBench), which contains over 1.7 million clips with a total duration of 11.8 thousand hours. We propose an automatic annotation pipeline to ensure each audible video has detailed descriptions for both its audio and video contents. We also introduce the Audio-Visual Harmoni score (AVHScore) to provide a quantitative measure of the alignment between the generated audio and video modalities. Additionally, we present a baseline model for TAVG called TAVDiffusion, which uses a two-stream latent diffusion model to provide a fundamental starting point for further research in this area. We achieve the alignment of audio and video by employing cross-attention and contrastive learning. Through extensive experiments and evaluations on TAVGBench, we demonstrate the effectiveness of our proposed model under both conventional metrics and our proposed metrics.

CCS CONCEPTS

• Computing methodologies → Image and video acquisition.

KEYWORDS

Text to Audible-Video Generation Benchmark (TAVGBench), Text to Audible-Video Diffusion (TAVDiffusion)

1 INTRODUCTION

The text to video generation task [2, 10, 13, 39, 47, 51] has been boosted through the integration of computer vision and natural language processing. This task translates textual descriptions into visual representations, enriching multimedia experiences, and improving accessibility for individuals with visual impairments. However, we observe that although existing methods excel in converting textual descriptions into visual content, the endeavor to integrate synchronized audio into these videos remains largely unexplored. This gap underscores a fundamental necessity within the realm of multimodal generation—the imperative to generate video content with auditory components guided solely by textual descriptions.

In this paper, considering the clear gap in current research, we introduce a new task: Text to Audible-Video Generation (TAVG). This task marks a significant change, requiring models to move beyond

just generating visual content and also creating audio alongside it. Unlike typical text to video tasks that only focus on unimodal video generation, TAVG requires generating both audio and video at the same time, guided by written descriptions. By taking on this task, we aim to push the boundaries of multimodal generation, making it possible to create immersive audio-visual experiences using only text prompts. The task definition is shown in Fig. 1.

To successfully achieve TAVG, a comprehensive dataset with well-aligned audio and video components is essential. However, we find no mature benchmark available for this task to support training and testing, primarily attributable to the absence of such a large-scale dataset. Building upon the foundation of TAVG, we propose establishing a Text to Audible-Video Generation Benchmark (TAVGBench), which allows the model to be trained in a supervised manner. At the core of TAVGBench lies a carefully selected dataset, comprising diverse textual descriptions and their corresponding audio-visual pairs. This dataset facilitates comprehensive evaluation and comparison of various methods. Our dataset consists of over 1.7 million audio-visual pairs sourced from YouTube videos. We design a coarse-to-fine pipeline to automatically achieve text annotation for audio-visual pairs in the dataset. Specifically, we utilize BLIP2 [23] and WavCaps [27] to describe the video and audio components, respectively. Additionally, we employ ChatGPT [29] to rephrase and integrate annotations from both modalities, which enables our annotation pipeline to excel in understanding context and producing human-like text descriptions. To evaluate the alignment degree between the generated audio and video, we introduce a new metric for the TAVG task to measure the harmony of the generated results, called the Audio-Visual Harmoni score (AVHScore). This metric quantifies the alignment between video and audio in a multi-modal, high-dimensional semantic space.

Utilizing our proposed TAVGBench, we present a Text to Audible-Video Diffusion (TAVDiffusion) model as the baseline method. This method is based on the latent diffusion model [34], representing an initial attempt to generate audio and video from text. Given the requirement of multimodal alignment, we propose two strategies to achieve the alignment of multimodal latent variables from the perspective of feature interaction and feature constraints. We extensively evaluate the baseline model against the proposed TAVGBench using both the conventional metrics and our proposed metrics and demonstrate the effectiveness of our method in the task of TAVG.

As follows, we summarize our main contributions as:

- We introduce the TAVG task, extending multimodal generation by integrating synchronized audio with visual content, addressing a crucial research gap.
- We present TAVGBench, a large-scale benchmark dataset with an automatic text description annotation pipeline and a novel Audio-Visual Harmoni score (AVHScore), significantly facilitating the TAVG task.
- We propose the Text to Audible-Video Diffusion (TAVDiffusion) model as a baseline method built upon the latent diffusion model.

Permission to make digital or hard copies of all or part of this work for personal or

Unpublished working draft. Not for distribution. distributed for profit or commercial advantage and that copies bear this notice and the full citation on the first page. Copyrights for components of this work owned by others than the author(s) must be honored. Abstracting with credit is permitted. To copy otherwise, or republish, to post on servers or to redistribute to lists, requires prior specific permission and/or a fee. Request permissions from permissions@acm.org.

ACM MM, 2024, Melbourne, Australia

© 2024 Copyright held by the owner/author(s). Publication rights licensed to ACM.

ACM ISBN 978-x-xxxx-xxxx-x/YY/MM

<https://doi.org/10.1145/nnnnnnn.nnnnnn>

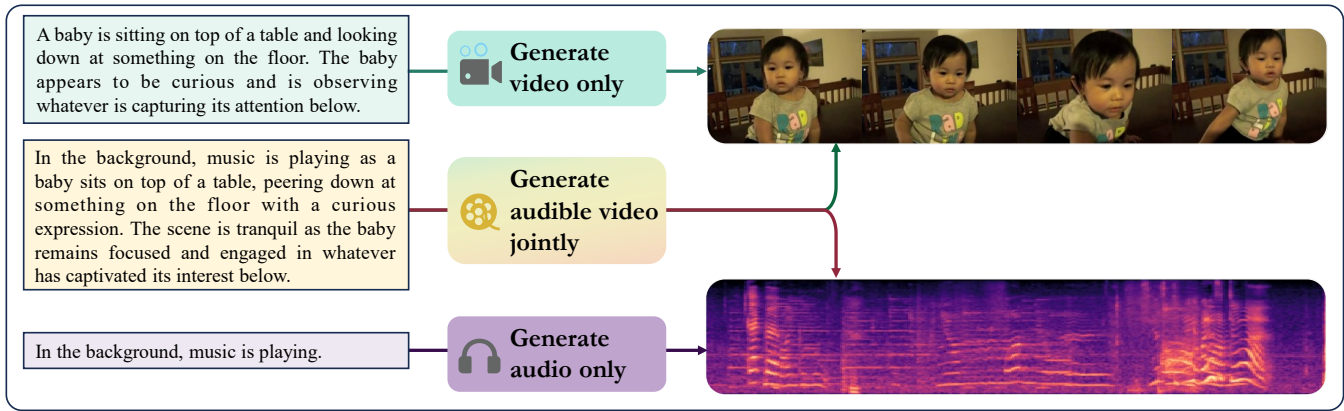


Figure 1: Comparison of the proposed TAVG task with existing generation tasks. (a) Text to video generation (TVG) generates the corresponding videos through text descriptions. (b) Text to audio generation (TAG) generates the corresponding audio through text descriptions. (c) The proposed TAVG task generates audio-visual content based on text descriptions of both audio and video elements.

2 RELATED WORK

Text to video generation. Text to video generation [2, 10, 13, 18, 39, 47, 49, 51] presents a challenging and extensively studied task. Previous studies utilize various generative models, such as GANs [24], and Autoregressive models [15, 55]. In recent years, the emergence of diffusion models [14] in content generation (*i.e.* text-to-image generation) catalyzes substantial advancements in text-to-video generation research. Imagen-Video [13], Make-A-Video [39], and show-1 [56] propose a deep cascade of temporal and spatial up-samplers for video generation, training their models jointly on both image and video datasets. The majority of subsequent works are grounded in the latent diffusion model [34], leveraging pre-trained UNet weights on 2D images. VideoLDM [2] adopts a latent diffusion model, where a pre-trained latent image generator and decoder are fine-tuned to ensure temporal coherence in generated videos. LAVIE [47] integrates Rotary Positional Encoding (RoPE) [42] into the network to capture temporal relationships among video frames. AnimateDiff [10] employs a strategy of freezing a pre-trained latent image generator while exclusively training a newly inserted motion modeling module. SimDA [51] proposes an efficient temporal adapter to help a trained 2D diffusion model extract temporal information. These advancements lay the foundation for an efficient multimodal diffusion pipeline.

Text to audio generation. Similar to video generation, the task of text to audio generation also evolves from GANs [28, 37] and Autoregressive models [20] to diffusion models. DiffSound [53] proposes a VQVAE model and a mask-based text generation strategy to address scarce audio-text paired data, albeit with potentially limited performance due to the lack of detailed text information. AudioGen [20] employs an autoregressive framework utilizing a Transformer-based decoder to generate tokens directly from the waveform. It applies data augmentation and simplifies language descriptions into labels, sacrificing detailed temporal and spatial information. AudioLDM [25] transfers the latent diffusion model from the domain of visual generation to text-to-audio generation. It

encodes text information through CLAP embedding [6] to achieve guidance. Tango [8] follows the LDM pipeline and replaces the CLAP to T5 [33] for more expressive text embedding.

Audio video mutual/joint generation. In addition to text-guided content generation, the mutual or joint generation of audio and video gradually become the focus of research in recent years. Typically, audio and video modalities serve as conditional signals for each other to achieve mutual generation, namely generating audio from video or video from audio. For the former, SpecVQGAN [16], CondFoleyGen [5], and Diff-Foley [26] implement audio generation from video using VQGAN, autoregressive transformer, and diffusion model, respectively. Regarding the latter, soundini [22] utilizes audio as a control signal to guide the video diffusion model for video editing purposes. Sung *et al.* [43] constrain the generated video content from audio to align more closely with the original audio using contrastive learning. TempoTokens [54] introduces an AudioMapper that employs a token encoded by a pre-trained audio encoder as a condition for enabling audio-to-video generation within a diffusion framework.

Based on the mutual generation of the two modalities, several studies explore the joint generation of audible video content. MM-diffusion [36] employs a diffusion UNet that takes inputs and outputs from both modalities, enabling the joint generation of two modalities for the first time. Zhu *et al.* [58] employ a video diffusion architecture to generate video and then retrieve audio, presenting an alternative approach to joint generation. Xing *et al.* [50] propose augmenting the existing diffusion model with optimization operations during the inference process to achieve audio-video generation while maintaining alignment.

Uniqueness of our benchmark. Despite the extensive exploration of multimodal generation tasks, there currently lacks a comprehensive benchmark and large-scale dataset specifically for the text to audible-video generation task. Addressing this gap, our solution offers a dataset for both training and evaluation, alongside metrics for assessing multimodal alignment. Additionally, we provide a straightforward baseline method.

Table 1: Statistics of TAVGBench and other existing video generation datasets. The terms “audio” and “video” represent the modality described by the description in the dataset. The terms “Sentence” and “Word” represent the average number of sentences and words per video annotation, respectively.

| Dataset | Sample | | Description | | | | | |
|----------------|--------|----------|-------------|-------|-------------------|----------|-------|--|
| | Clip | DUR. (h) | Audio | Video | Method | Sentence | Word | |
| AudioCaps [19] | 46K | 5.3 | ✓ | ✗ | Human-written | 1.0 | 9.03 | |
| MSR-VTT [52] | 10K | 41.2 | ✗ | ✓ | Human-written | 20.0 | 185.7 | |
| WebVid [1] | 10M | 53K | ✗ | ✓ | Automatic caption | 1.0 | 12.0 | |
| FAVDBench [38] | 11.4K | 24.4 | ✓ | ✓ | Human-written | 12.6 | 218.9 | |
| TAVGBench | 1.7M | 11.8K | ✓ | ✓ | Automatic caption | 2.32 | 49.98 | |

3 THE TAVGBENCH

3.1 Dataset statistics

The TAVG task entails the generation of audible videos guided by input text prompts. To support this task, we introduce a benchmark named TAVGBench. Our dataset is sourced from AudioSet [7], comprising 2 million aligned audio-video pairs obtained from YouTube. After excluding invalid videos, we obtained 1.7 million pieces of original data. Each video sample has a duration of 10 seconds, contributing to a total video duration of 11.8K hours in the dataset. To provide a comprehensive understanding of the scale and characteristics of our dataset, we compare it with the datasets from other related tasks. Table 1 presents a comparative analysis of TAVGBench against these datasets in terms of size, source, and other relevant attributes.

It can be observed from Table 1 that the AudioCaps [19], MSR-VTT [52], and WebVid [1] only describe the content of a single modality (only audio or video modality). Although FAVDBench describes two modalities, the scale of the dataset is limited. The TAVGBench that we propose takes into account descriptions of both audio and video modalities while ensuring a sufficiently large dataset scale. In addition, the videos in WebVid have watermarks, which greatly restrict their application in actual scenarios. This comparison highlights the scale and unique characteristics of the TAVGBench dataset, emphasizing its potential for advancing research in audible-video generation. Additionally, TAVGBench exhibits a balanced distribution of textual descriptions, with an average of 2.32 sentences and 49.98 words per video annotation, providing substantial contextual information for each clip. These comparative statistics underscore TAVGBench’s extensive scale, multimodal nature, and linguistic richness, positioning it as a valuable resource for advancing research in our TAVG task.

3.2 Annotation details

Given the absence of detailed text annotations in AudioSet [7] for both its video and audio content, we implement a coarse-to-fine pipeline to automate the generation of text descriptions. The complete pipeline is shown in Fig. 2. Initially, we employ two sophisticated methods, namely BLIP2 [23] for video description and WavCaps [27] for audio description, to annotate the video and audio components, respectively.

However, despite the effectiveness of these methods in capturing the essence of video and audio content, the generated annotations often lacked coherence and context. To address this limitation and

improve the overall quality of the annotations, we introduced a refinement step using ChatGPT [29], a powerful language model capable of paraphrasing and enriching textual input.

During the refinement phase, we utilize ChatGPT to rephrase and enhance the annotations generated by BLIP2 and WavCaps. By feeding the initial annotations into the ChatGPT model, we obtain revised annotations that exhibit enhanced coherence, contextual relevance, and linguistic refinement. Initially, we individually rephrase the video and audio descriptions to rectify grammatical errors and enhance descriptive content. Subsequently, we employ ChatGPT to amalgamate the descriptions from both modalities into a unified, coherent sentence. This iterative process not only enhances the readability of the annotations but also ensures consistency and accuracy throughout the entire annotation corpus.

Incorporating ChatGPT into our pipeline has significantly enhanced the ability to detect subtle nuances and semantic complexities within the video and audio content. As a result, our annotation pipeline excels in understanding context and producing human-like text descriptions, thus facilitating the creation of annotations that more precisely capture the essence of the underlying content.

3.3 Evaluation metric

Existing metrics for video (FVD, KVD [45]) and audio (FAD [36]) generation primarily focus on the quality of each modality separately. However, for The TAVG task, we not only need to generate high-quality audio and video but also need to ensure that these two modalities are accurately synchronized. To address the necessity for evaluating the alignment degree between generated audio and video, we propose a novel metric called the Audio-Visual Harmony Score (AVHScore). This metric quantifies the alignment of audio-video pairs by calculating the product of the extracted audio-visual features. We use a robust feature extractor (ImageBind [9]) to project the video frames and the audio into a unified feature space. Formally, we define the AVHScore S_{AVH} as follows:

$$S_{AVH} = \frac{1}{n} \sum_{i=1}^N \cos(E_v(V_i), E_a(A)) \quad (1)$$

where \cos denotes cosine similarity. E_v and E_a represent the vision encoder and audio encoder, respectively, in the ImageBind model. N signifies the number of video frames, and we compute the similarity between each video frame and the corresponding audio input, averaging the results across all frames.

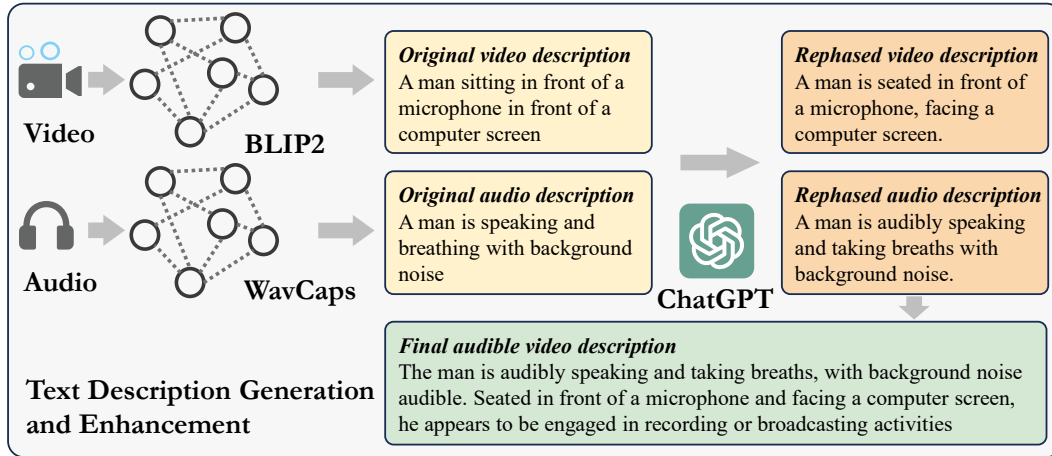


Figure 2: Overview of the annotation pipeline. We employ BLIP2 for video descriptions and WavCaps for audio descriptions. The descriptions are further refined using ChatGPT, resulting in the final detailed audible video description.



Figure 3: Data samples. The video (we give three frames for each video clip), audio, and the corresponding generated captions. We highlight the video caption in black and the audio caption in blue.

4 A BASELINE

We propose a new baseline method for the text to audible-video generation (TAVG) task as shown in Fig. 4, named TAVDiffusion. The entire network structure is based on the latent diffusion model [34].

4.1 Preliminary: Latent diffusion model

The latent diffusion model follows the standard formulation outlined in DDPM [14], which comprises a forward diffusion process and a backward reverse denoising process. Initially, a data sample $\mathbf{x} \sim p(\mathbf{x})$ undergoes processing by an autoencoder, consisting of an encoder \mathcal{E} and a decoder \mathcal{D} . The autoencoder projects \mathbf{x} into a latent variable \mathbf{z} via $\mathbf{z} = \mathcal{E}(\mathbf{x})$. Subsequently, the diffusion and

denoising process takes place within the latent space. The denoised latent variable is recovered to the input space by $\hat{\mathbf{x}} = \mathcal{D}(\hat{\mathbf{z}}_0)$.

Inspired by non-equilibrium thermodynamics, diffusion models [14, 40] are a class of latent variable (z_1, \dots, z_T) models of the form $p_\theta(z_0) = \int p_\theta(z_{0:T}) dz_{1:T}$, where the latent variables are of the same dimensionality as the input data z_0 . The joint distribution $p_\theta(z_{0:T})$ is also called the *reverse process*:

$$p_\theta(z_{0:T}) = p_\theta(z_T) \prod_{t=1}^T p_\theta(z_{t-1}|z_t), \quad (2)$$

where

$$p_\theta(z_{t-1}|z_t) = \mathcal{N}(z_{t-1}; \mu_\theta(z_t, t), \Sigma_\theta(z_t, t)). \quad (3)$$

Here, μ_θ and Σ_θ are determined through a denoiser network $\epsilon_\theta(z_t, t)$, typically structured as a UNet [35].

The approximate posterior $q(z_{1:T}|z_0)$ is called the *forward process*, which is fixed to a Markov chain that gradually adds noise according to a predefined noise scheduler $\beta_{1:T}$:

$$q(z_{1:T}|z_0) = \prod_{t=1}^T q(z_t|z_{t-1}), \quad (4)$$

where

$$q(z_t|z_{t-1}) = \mathcal{N}(z_t; \sqrt{1 - \beta_t} z_{t-1}, \beta_t \mathbf{I}). \quad (5)$$

The training is performed by minimizing a variational bound on negative log-likelihood:

$$\begin{aligned} \mathbb{E}_q[-\log p_\theta(z_0)] &\leq \mathbb{E}_q[-\log \frac{p_\theta(z_{0:T})}{q(z_{1:T}|z_0)}] \\ &= \mathbb{E}_q[D_{KL}(q(z_T|z_0) \| p(z_T))] \\ &\quad + \sum_{t>1} D_{KL}(q(z_{t-1}|z_t, z_0) \| p_\theta(z_{t-1}|z_t)) \\ &\quad - \log p_\theta(z_0|z_1). \end{aligned} \quad (6)$$

Hence, the final training objective of θ is a noise estimation loss, with a conditional variable \mathbf{c} , it can be formulated as:

$$\mathcal{L}_{\text{diffusion}}(\theta) := \mathbb{E}_{\mathbf{z}, \mathbf{c}, \epsilon \sim \mathcal{N}(0, \mathbf{I}), t} [\|\epsilon - \epsilon_\theta(\mathbf{z}_t, \mathbf{c}, t)\|^2]. \quad (7)$$

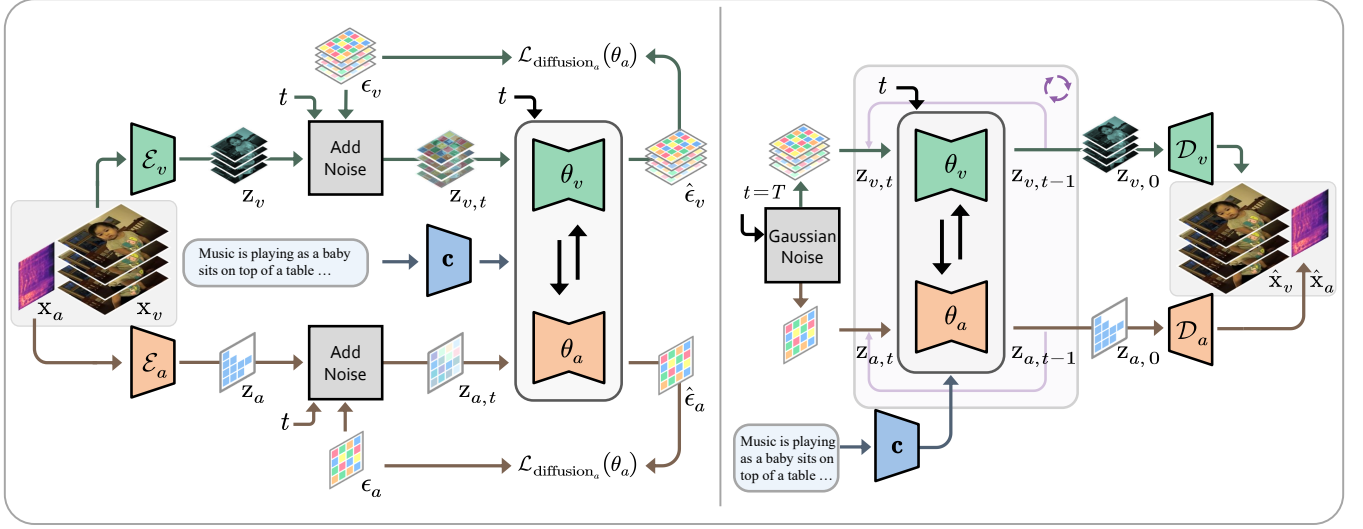


Figure 4: Overview of the TAVDiffusion training (left) and inference (right) stages. We develop a two-stream architecture. During the training phase, we randomly select a timestep t and employ diffusion loss to guide the single-step denoising. In the inference phase, iterative denoising is conducted to finally produce an audible video.

4.2 TAVDiffusion

With the forward and reverse process in the latent diffusion model defined in Sec. 4.1, we further present the baseline two-stream diffusion pipeline for joint text to audible-video diffusion.

Multimodal Latent encoders. We employ two independent latent autoencoders for our multimodal input to conduct latent space encoding and decoding. This process can be formulated as:

$$\begin{aligned} \text{Encoder: } \mathbf{z}_a &= \mathcal{E}_a(\mathbf{x}_a), \mathbf{z}_v = \mathcal{E}_v(\mathbf{x}_v), \\ \text{Decoder: } \hat{\mathbf{x}}_a &= \mathcal{D}_a(\hat{\mathbf{z}}_{a,0}), \hat{\mathbf{x}}_v = \mathcal{D}_v(\hat{\mathbf{z}}_{v,0}), \end{aligned} \quad (8)$$

where the subscripts a and v represent audio and video modality, respectively. Specifically, for \mathcal{D}_v , we utilize the pre-trained autoencoder in stable diffusion [34] along with its weights. Given an original video with dimensions $T \times 3 \times H_v \times W_v$, the size of the latent variable becomes $T \times 4 \times \frac{H_v}{8} \times \frac{W_v}{8}$. As for \mathcal{D}_a , we employ the pre-trained autoencoder from AudioLDM [25] to encode the audio mel spectrogram into the latent space. For the dimensions $1 \times H_a \times W_a$ of the input mel spectrogram, the size of the latent variable becomes $8 \times \frac{H_a}{8} \times \frac{W_a}{8}$.

Multimodal diffusion process. For the input of audio and video modalities, we use a two-stream structure to perform the forward and reverse diffusion process for the latent variables $\mathbf{z}_a, \mathbf{z}_v$, as shown in Fig. 4. Unlike vanilla diffusion where a single modality is generated, we aim to simultaneously recover two consistent modalities (*i.e.* audio and video) within a single diffusion process.

We consider that the reverse and forward processes of each modality are independent because they have distinct distributions. Taking the audio latent variable \mathbf{z}_a as an illustration, its reverse process at timestep t is defined as:

$$p_{\theta_a}(\mathbf{z}_{a,t-1}|\mathbf{z}_t) = \mathcal{N}(\mathbf{z}_{a,t-1}; \mu_{\theta_a}(\mathbf{z}_{a,t}, t), \Sigma_{\theta_a}(\mathbf{z}_{a,t}, t)). \quad (9)$$

The forward process at timestep t is defined as follows:

$$q(\mathbf{z}_{a,t}|\mathbf{z}_{a,t-1}) = \mathcal{N}(\mathbf{z}_{a,t}; \sqrt{1 - \beta_t}\mathbf{z}_{a,t-1}, \beta_t\mathbf{I}). \quad (10)$$

For brevity, we omit the reverse and forward process for video \mathbf{z}_v via θ_v , as it shares a similar formulation. It is important to note that we empirically set a shared schedule for hyper-parameters β across audio and video to streamline the process definition.

Summarizing the formulations above, the final definition of the multimodal diffusion loss is:

$$\begin{aligned} \mathcal{L}_{\text{diffusion}}(\theta_a, \theta_v) &= \mathcal{L}_{\text{diffusion}_a}(\theta_a) + \mathcal{L}_{\text{diffusion}_v}(\theta_v) \\ &:= \mathbb{E}_{\mathbf{z}_a, \mathbf{c}, \epsilon_a \sim \mathcal{N}(0, \mathbf{I}), t} \left[\|\epsilon_a - \epsilon_{\theta_a}(\mathbf{z}_{a,t}, \mathbf{c}, t)\|^2 \right] \\ &\quad + \mathbb{E}_{\mathbf{z}_v, \mathbf{c}, \epsilon_v \sim \mathcal{N}(0, \mathbf{I}), t} \left[\|\epsilon_v - \epsilon_{\theta_v}(\mathbf{z}_{v,t}, \mathbf{c}, t)\|^2 \right]. \end{aligned} \quad (11)$$

In our task, the conditional variable \mathbf{c} denotes the text embedding of the input, and we use the CLIP [32] text encoder with its tokenizer to obtain the text embedding.

Diffusion UNet architecture. For θ_a and θ_v , we employ two parallel UNet branches to perform denoising for audio and video latent variables, respectively. For the audio UNet θ_a , we directly utilize the UNet architecture from stable diffusion [34] and adjust the number of channels in its input layer from 4 to 8. Regarding the video UNet θ_v , akin to AnimateDiff [10], we adapt the 2D convolution in the 2D UNet of stable diffusion¹ to a pseudo-3D convolution, which comprises a 1D convolution followed by a 2D convolution. Additionally, we incorporate the Temporal Transformer layer [46] into the network. These changes allow the network to accept video as input and keep its temporal details.

4.3 Multimodal interaction

In this section, we introduce a methodology for aligning the intermediate features f_a, f_v , associated with θ_a, θ_v respectively, by

¹We use stable diffusion version 1.5 and its pre-trained weights as partial initialization.

employing a cross-attention mechanism [46]. Our approach aims to enhance the performance of joint generation tasks involving video and audio by synchronizing the information flow between the two modalities during the diffusion process. Given f_a and f_v , we represent the process of cross-attention as follows and utilize the resulting \hat{f}_a and \hat{f}_v as the input of the diffusion UNet decoder.

$$\hat{f}_a = \text{CrossAtten}(f_a, f_v), \hat{f}_v = \text{CrossAtten}(f_v, f_a). \quad (12)$$

4.4 Multimodal alignment

The feature interaction mechanism does not explicitly enforce the alignment of multimodal features. Hence, it is crucial to integrate a loss function that guarantees alignment between the feature representations of audio and visual modalities. To tackle this issue, we propose an Explicit audio-visual Alignment Strategy (EAS) based on contrastive learning [11].

In a multimodal scenario, where we have feature vectors (\hat{f}_a, \hat{f}_v) representing two modalities, contrastive learning is employed to model the alignment between these modalities. The underlying assumption is that features that align well with each other should be brought closer together, whereas those that contradict each other should be pushed apart. We define alignment as a bidirectional process, leading to the formulation of the contrastive loss as follows:

$$\begin{aligned} \mathcal{L}_{\text{EAS}}(\hat{f}_a, \hat{f}_v) = & -\log \frac{\exp(s(\hat{f}_a, \hat{f}_a^p)/\tau)}{\sum_{\hat{f}_v} \exp(s(\hat{f}_a, \hat{f}_v)/\tau)} \\ & -\log \frac{\exp(s(\hat{f}_v, \hat{f}_v^p)/\tau)}{\sum_{\hat{f}_a} \exp(s(\hat{f}_v, \hat{f}_a)/\tau)}, \end{aligned} \quad (13)$$

where $\tau = 0.1$ is the temperature scalar, \hat{f}_a^p (\hat{f}_v^p) is the positive sample corresponding to \hat{f}_a (\hat{f}_v) from the other modality. The function $s(\cdot, \cdot)$ computes the cosine similarity. We generate positive and negative samples based on the feature representations of two modalities. Specifically, we define embeddings of the two modalities with the same index (paired data) as positive samples, while those with different indexes are considered negative samples (unpaired data).

The bottleneck of contrastive learning lies in designing the positive/negative pairs with effective similarity measure, *i.e.* $s(\cdot, \cdot)$ in our case. We use a linear projection with softmax activation $l_\beta(\cdot)$ to calculate similarity weight based on the input of a specific modality [4] different information contained in different tokens. Given two modalities (a, v), a weighted similarity function $s(\cdot, \cdot)$ is:

$$s(\hat{f}_a, \hat{f}_v) = \sum_{\hat{f}_a} l_{\beta_a}(\hat{f}_a) \cos(\hat{f}_a, \hat{f}_v) + \sum_{\hat{f}_v} l_{\beta_v}(\hat{f}_v) \cos(\hat{f}_v, \hat{f}_a). \quad (14)$$

4.5 Objective Function

The objective functions are divided into task loss ($\mathcal{L}_{\text{diffusion}}$) and feature alignment loss (\mathcal{L}_{EAS}). The total loss is a weighted sum of the above terms:

$$\mathcal{L} = \mathcal{L}_{\text{diffusion}} + \lambda \mathcal{L}_{\text{EAS}}, \quad (15)$$

where λ represents the balanced weights during training. Empirically, the loss weight is set as $\lambda = 0.1$.

5 EXPERIMENTAL RESULTS

5.1 Implementation details

Datasets. We train our model on the TAVGBench dataset that we introduced. For the evaluation phase, we select 3,000 samples from the TAVGBench evaluation subset. Additionally, we evaluate the performance of our model on the test subset of FAVDBench [38], which comprises 1,000 samples. The FAVDBench provides more fine-grained audible video descriptions, enabling the generation of more detailed videos. Importantly, because the data of FAVDBench is not utilized in the training phase, we could assess the *zero-shot* capabilities of our model based on its performance on FAVDBench. **Training Details.** We implement TAVDiffusion using PyTorch [30]. We adopt a video training resolution of $256 \times 320 \times 20$ to balance training efficiency and motion quality. We convert the audio into a mel spectrogram and perform training and inference on it. We use the MelGAN Vocoder [21] to convert the denoised audio mel spectrogram into the audio waveform. We use a learning rate of 1×10^{-4} and train the model with 64 NVIDIA A100 GPUs for 1.0×10^5 steps. At inference time, we apply the DDIM scheduler [41] and only sample 50 timesteps.

Evaluation Metrics. We begin by separately measuring the quality of the generated audio and video. To evaluate the video, we adopt the Frechet Video Distance (FVD) [45], Kernel Video Distance (KVD) [44], and CLIPSIM [12, 48] metrics. FVD and KVD employ the I3D [3] classifier pre-trained on the Kinetics-400 dataset [17]. For audio evaluation, we employ FAD [36] to gauge the distance between the features of the generated audio and the reference audio. We also use our proposed AVHScore to measure the alignment degree of the generated results. For all evaluations, we generate a random sample for each text without any automatic ranking.

5.2 Main results

Comparison methods setting. To the best of our knowledge, there are no existing usable methods directly relevant to our proposed task for comparison. Therefore, we combine existing related models and design two-stage methods for comparison.

- (1) AnimateDiff [10]+AudioLDM [25]: Input text and utilize these two models to generate audio and video respectively.
- (2) AnimateDiff [10]+Diff-Foley [26]: Input text, employ AnimateDiff to generate video, and subsequently utilize Diff-Foley to generate audio based on the video.
- (3) AudioLDM [25]+TempoToken [54]: Input text, use AudioLDM to generate audio, and then employ TempoToken to generate video based on the audio.

Quantitative comparison. We present the quantitative results of our method alongside comparison methods for the TAVGBench and FAVDBench datasets in Table 2. The results demonstrate that our TAVDiffusion model outperforms all comparisons in terms of video and audio quality metrics. Specifically, the scores for FVD and KVD are 776.25 and 65.53, respectively, while the FAD score is 1.46. This demonstrates significant consistency between the audible video we generated and the original content and is of higher quality. These results underscore a significant consistency between the videos generated by our model and the original content, indicating superior quality. Additionally, our model achieves a notable CLIPSIM score (24.18), reinforcing the semantic coherence between the generated

Table 2: Quantitative comparison. The numbers in the left column of the table represent the comparison methods we described in the previous section.

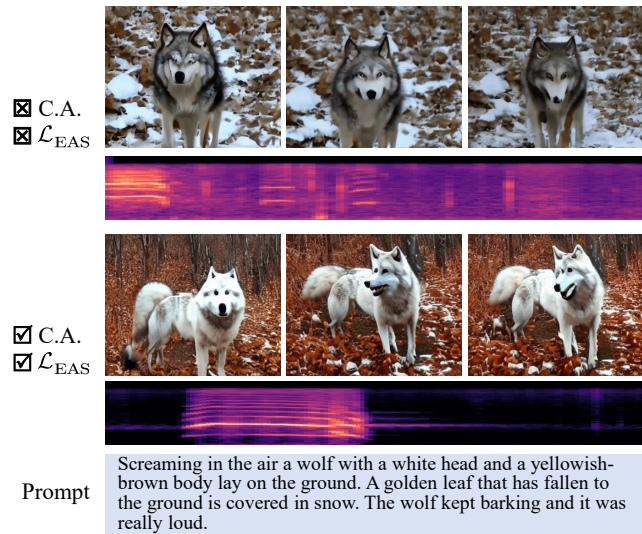
| Methods | TAVGBench | | | | | FAVDBench [38] | | | | |
|---------|---------------|--------------|--------------|-------------|--------------|----------------|---------------|--------------|-------------|--------------|
| | FVD ↓ | KVD ↓ | CLIPSIM ↑ | FAD ↓ | AVHScore ↑ | FVD ↓ | KVD ↓ | CLIPSIM ↑ | FAD ↓ | AVHScore ↑ |
| (1) | 777.54 | 70.04 | 22.49 | 1.62 | 10.17 | 867.58 | 115.81 | 22.11 | 1.67 | 12.13 |
| (2) | 777.54 | 70.04 | 22.49 | 1.81 | 12.28 | 867.58 | 115.81 | 22.11 | 1.89 | 15.07 |
| (3) | 1624.81 | 88.61 | 14.87 | 2.12 | 6.38 | 2640.96 | 591.43 | 15.16 | 2.29 | 6.12 |
| Ours | 516.56 | 45.76 | 25.44 | 1.38 | 23.35 | 776.25 | 104.26 | 24.18 | 1.46 | 29.06 |



Figure 5: Qualitative comparison. We compare our TAVDiffusion model with methods (1) and (2). Given the inferior visual quality of method (3) in our task (see Table 2), we exclude it from the qualitative comparison. Best viewed on screen.

Table 3: Ablation studies. “C.A.” represents cross-attention mechanism, and \mathcal{L}_{EAS} represents our proposed explicit audio-visual alignment strategy.

| C.A. | \mathcal{L}_{EAS} | TAVGBench | | | | | FAVDBench [38] | | | | |
|------|---------------------|---------------|--------------|--------------|-------------|--------------|----------------|---------------|--------------|-------------|--------------|
| | | FVD ↓ | KVD ↓ | CLIPSIM ↑ | FAD ↓ | AVHScore ↑ | FVD ↓ | KVD ↓ | CLIPSIM ↑ | FAD ↓ | AVHScore ↑ |
| ✗ | ✗ | 687.23 | 66.21 | 23.02 | 1.58 | 14.59 | 843.19 | 112.07 | 22.58 | 1.62 | 14.67 |
| ✗ | ✓ | 614.28 | 59.23 | 23.89 | 1.46 | 18.69 | 819.54 | 109.21 | 22.64 | 1.54 | 19.76 |
| ✓ | ✗ | 589.71 | 51.44 | 24.68 | 1.51 | 19.88 | 791.57 | 106.95 | 23.98 | 1.51 | 20.59 |
| ✓ | ✓ | 516.56 | 45.76 | 25.44 | 1.38 | 23.35 | 776.25 | 104.26 | 24.18 | 1.46 | 29.06 |

**Figure 6: Qualitative comparison for the ablation studies. Best viewed on screen.**

videos and their associated prompts. Significantly, our model attains an AVHScore of 29.06, further evidencing its ability to generate videos with closely aligned audio and visual components. Note that neither our model nor the comparison models were exposed to the FAVDBench data during the training phase, thereby the results on this dataset further underscore our zero-shot capabilities.

Qualitative comparison. In Fig. 5, we present qualitative results comparing our method to the compared generators. The figure illustrates that TAVDiffusion outperforms the comparison models in terms of visual fidelity and the alignment of text, video, and audio. In the first example, the “performer” created by TAVDiffusion displays significantly enhanced realism, especially in facial expressions and hand movements. The generated audio also follows the two elements “guitar sound” and “singing voice” in the prompt. In the second example, TAVDiffusion showcases its ability to produce complex real-life scenes, maintaining the precise shapes of essential objects. It skillfully navigates the dynamics between the foreground object (e.g. the car) and the background scene, complemented by realistic audio. We also showcase our model’s performance in two distinct scenarios: environments with significant background noise and notably quieter environments. For the former, our model generates various types of audio, such as music and human cheers, as directed by the prompt. For the latter, our model uniquely and accurately produces the sound of “birds chirping”. This comparison shows the versatility of the model, demonstrating its effectiveness across a broad spectrum of audio-visual scenes. By evaluating the

model in such contrasting settings, we highlight its universal applicability and robustness in processing diverse auditory and visual inputs. We sincerely hope the readers find more examples of audible videos in the supplementary materials.

5.3 Ablation studies

To demonstrate the effectiveness of our proposed modules, we conduct ablation studies from both quantitative metrics (see Table 3) and qualitative visualizations (see Fig. 6). In Table 3, it is evident that the two strategies we proposed, multimodal cross-attention and multimodal alignment, enhance both the quality of video and audio generation and the alignment score. In Fig. 6, we can observe that the “wolf” produced by our final model appears more realistic than that of the comparisons, with its mouth movements accurately reflecting the “kept barking” prompt and the generated audio. Please refer to the supplementary material for more samples.

5.4 Potential applications

Our TAVGBench and baseline model TAVDiffusion have a wide range of multimedia application fields. Our dataset, which includes large-scale video, audio, and corresponding text descriptions, is well-suited for a diverse range of multimodal tasks. It allows for the simultaneous use of text and audio as prompts to generate videos. Additionally, TAVGBench can be used to train audible video captioning models [38, 57] can substantially reduce the impact of insufficient audio-video-text data pairs as mentioned in [38].

6 CONCLUSION

We explored the challenge of creating videos with matching audio from text descriptions, a task known as Text to Audible-Video Generation (TAVG). To aid in this research, we introduced a new benchmark called TAVGBench, filled with over 1.7 million video clips. This resource is designed to help improve and evaluate TAVG models. We developed a method to automatically describe each audio-visual element, ensuring detailed and useful annotations for researchers. A new metric called Audio-Visual Harmoni score (AVH-Score) was designed to evaluate the alignment of generated audible video. We introduced TAVDiffusion, a baseline model leveraging latent diffusion. This model incorporates cross-attention and contrastive learning mechanisms to achieve audio-visual alignment within the diffusion UNet framework. Extensive experimental results verified the effectiveness of our proposed framework, thus opening new avenues for multimedia content creation. In the future, we aim to explore a multimodal diffusion transformer [31] to facilitate audible video generation through a unified architecture.

REFERENCES

- [1] Max Bain, Arsha Nagrani, Gül Varol, and Andrew Zisserman. 2021. Frozen in time: A joint video and image encoder for end-to-end retrieval. In *International Conference on Computer Vision (ICCV)*. 1728–1738.
- [2] Andreas Blattmann, Robin Rombach, Huan Ling, Tim Dockhorn, Seung Wook Kim, Sanja Fidler, and Karsten Kreis. 2023. Align your latents: High-resolution video synthesis with latent diffusion models. In *Conference on Computer Vision and Pattern Recognition (CVPR)*. 22563–22575.
- [3] Joao Carreira and Andrew Zisserman. 2017. Quo vadis, action recognition? a new model and the kinetics dataset. In *Conference on Computer Vision and Pattern Recognition (CVPR)*. 6299–6308.
- [4] Sihan Chen, Xingjian He, Longteng Guo, Xinxin Zhu, Weining Wang, Jinghui Tang, and Jing Liu. 2023. Valor: Vision-audio-language omni-perception pretraining model and dataset. *arXiv preprint arXiv:2304.08345* (2023).
- [5] Yuexi Du, Ziyang Chen, Justin Salamon, Bryan Russell, and Andrew Owens. 2023. Conditional generation of audio from video via foley analogies. In *Conference on Computer Vision and Pattern Recognition (CVPR)*. 2426–2436.
- [6] Benjamin Elizalde, Soham Deshmukh, Mahmoud Al Ismail, and Huaming Wang. 2023. Clap learning audio concepts from natural language supervision. In *IEEE International Conference on Acoustics, Speech and Signal Processing (ICASSP)*. IEEE, 1–5.
- [7] Jort F Gemmeke, Daniel PW Ellis, Dylan Freedman, Aren Jansen, Wade Lawrence, R Channing Moore, Manoj Plakal, and Marvin Ritter. 2017. Audio set: An ontology and human-labeled dataset for audio events. In *IEEE International Conference on Acoustics, Speech and Signal Processing (ICASSP)*. IEEE, 776–780.
- [8] Deepanway Ghosal, Navonil Majumder, Ambuj Mehrish, and Soujanya Poria. 2023. Text-to-audio generation using instruction-tuned llm and latent diffusion model. *arXiv preprint arXiv:2304.13731* (2023).
- [9] Rohit Girdhar, Alaeldin El-Nouby, Zhuang Liu, Mannat Singh, Kalyan Vasudev Alwala, Armand Joulin, and Ishan Misra. 2023. Imagebind: One embedding space to bind them all. In *Conference on Computer Vision and Pattern Recognition (CVPR)*. 15180–15190.
- [10] Yuwei Guo, Ceyuan Yang, Anyi Rao, Zhengyang Liang, Yaohui Wang, Yu Qiao, Maneesh Agrawala, Dahua Lin, and Bo Dai. 2023. AnimateDiff: Animate Your Personalized Text-to-Image Diffusion Models without Specific Tuning. In *International Conference on Learning Representations (ICLR)*.
- [11] Kaiming He, Haoqi Fan, Yuxin Wu, Saining Xie, and Ross Girshick. 2020. Momentum contrast for unsupervised visual representation learning. In *Conference on Computer Vision and Pattern Recognition (CVPR)*. 9729–9738.
- [12] Jack Hessel, Ari Holtzman, Maxwell Forbes, Roman Le Bras, and Yejin Choi. 2021. CLIPScore: A Reference-free Evaluation Metric for Image Captioning. In *Conference on Empirical Methods in Natural Language Processing (EMNLP)*. 7514–7528.
- [13] Jonathan Ho, William Chan, Chitwan Saharia, Jay Whang, Ruiqi Gao, Alexey Gritsenko, Diederik P Kingma, Ben Poole, Mohammad Norouzi, David J Fleet, et al. 2022. Imagen video: High definition video generation with diffusion models. *arXiv preprint arXiv:2210.02303* (2022).
- [14] Jonathan Ho, Ajay Jain, and Pieter Abbeel. 2020. Denoising diffusion probabilistic models. *Conference on Neural Information Processing Systems (NeurIPS)* (2020), 6840–6851.
- [15] Wenyi Hong, Ming Ding, Wendi Zheng, Xinghan Liu, and Jie Tang. 2022. CogVideo: Large-scale Pretraining for Text-to-Video Generation via Transformers. In *International Conference on Learning Representations (ICLR)*.
- [16] Vladimir Iashin and Esa Rahtu. 2021. Taming Visually Guided Sound Generation. In *British Machine Vision Conference (BMVC)*. BMVA Press.
- [17] Will Kay, Joao Carreira, Karen Simonyan, Brian Zhang, Chloe Hillier, Sudheendra Vijayanarasimhan, Fabio Viola, Tim Green, Trevor Back, Paul Natsev, et al. 2017. The kinetics human action video dataset. *arXiv preprint arXiv:1705.06950* (2017).
- [18] Levon Khachatryan, Andranik Movsisyan, Vahram Tadevosyan, Roberto Henschel, Zhangyang Wang, Shant Navasardyan, and Humphrey Shi. 2023. Text2video-zero: Text-to-image diffusion models are zero-shot video generators. In *International Conference on Computer Vision (ICCV)*. 15954–15964.
- [19] Chris Dongjoo Kim, Byeongchang Kim, Hyunmin Lee, and Gunhee Kim. 2019. AudioCaps: Generating Captions for Audios in The Wild. In *NAACL-HLT*.
- [20] Felix Kreuk, Gabriel Synnaeve, Adam Polyak, Uriel Singer, Alexandre Défossez, Jade Copet, Devi Parikh, Yaniv Taigman, and Yossi Adi. 2022. AudioGen: Textually Guided Audio Generation. In *International Conference on Learning Representations (ICLR)*.
- [21] Kundan Kumar, Rithesh Kumar, Thibault De Boissiere, Lucas Gestin, Wei Zhen Teoh, Jose Sotelo, Alexandre De Brebisson, Yoshua Bengio, and Aaron C Courville. 2019. Melgan: Generative adversarial networks for conditional waveform synthesis. *Conference on Neural Information Processing Systems (NeurIPS)* 32 (2019).
- [22] Seung Hyun Lee, Sieun Kim, Innfarn Yoo, Feng Yang, Donghyeon Cho, Youngseo Kim, Huiwen Chang, Jinkyu Kim, and Sangpil Kim. 2023. Soundini: Sound-guided diffusion for natural video editing. *arXiv preprint arXiv:2304.06818* (2023).
- [23] Junnan Li, Dongxu Li, Silvio Savarese, and Steven Hoi. 2023. Blip-2: Bootstrapping language-image pre-training with frozen image encoders and large language models. In *International Conference on Machine Learning (ICML)*. PMLR, 19730–19742.
- [24] Yitong Li, Martin Min, Dinghan Shen, David Carlson, and Lawrence Carin. 2018. Video generation from text. In *AAAI Conference on Artificial Intelligence (AAAI)*, Vol. 32.
- [25] Haohe Liu, Zehua Chen, Yi Yuan, Xinhao Mei, Xubo Liu, Danilo Mandic, Wenwu Wang, and Mark D Plumbley. 2023. AudioLDM: Text-to-Audio Generation with Latent Diffusion Models. In *International Conference on Learning Representations (ICLR)*. PMLR, 21450–21474.
- [26] Simian Luo, Chuhan Yan, Chenxu Hu, and Hang Zhao. 2024. Diff-foley: Synchronized video-to-audio synthesis with latent diffusion models. *Conference on Neural Information Processing Systems (NeurIPS)* 36 (2024).
- [27] Xinhao Mei, Chutong Meng, Haohe Liu, Qiuqiang Kong, Tom Ko, Chengqi Zhao, Mark D Plumbley, Yuxian Zou, and Wenwu Wang. 2023. Wavcaps: A chatgpt-assisted weakly-labelled audio captioning dataset for audio-language multimodal research. *arXiv preprint arXiv:2303.17395* (2023).
- [28] Javier Nistal, Stefan Lattner, and Gael Richard. 2020. Drumgan: Synthesis of drum sounds with timbral feature conditioning using generative adversarial networks. *arXiv preprint arXiv:2008.12073* (2020).
- [29] OpenAI. 2022. ChatGPT: OpenAI’s Conversational AI. <https://openai.com/chatgpt>.
- [30] Adam Paszke, Sam Gross, Francisco Massa, Adam Lerer, James Bradbury, Gregory Chanan, Trevor Killeen, Zeming Lin, Natalia Gimelshein, Luca Antiga, et al. 2019. Pytorch: An imperative style, high-performance deep learning library. *Conference on Neural Information Processing Systems (NeurIPS)* 32 (2019).
- [31] William Peebles and Saining Xie. [n. d.]. Scalable diffusion models with transformers.
- [32] Alec Radford, Jong Wook Kim, Chris Hallacy, Aditya Ramesh, Gabriel Goh, Sandhini Agarwal, Girish Sastry, Amanda Askell, Pamela Mishkin, Jack Clark, et al. 2021. Learning transferable visual models from natural language supervision. In *International Conference on Machine Learning (ICML)*, 8748–8763.
- [33] Colin Raffel, Noam Shazeer, Adam Roberts, Katherine Lee, Sharan Narang, Michael Matena, Yanqi Zhou, Wei Li, and Peter J Liu. 2020. Exploring the limits of transfer learning with a unified text-to-text transformer. *Journal of Machine Learning Research (JMLR)* 21, 140 (2020), 1–67.
- [34] Robin Rombach, Andreas Blattmann, Dominik Lorenz, Patrick Esser, and Björn Ommer. 2022. High-resolution image synthesis with latent diffusion models. In *Conference on Computer Vision and Pattern Recognition (CVPR)*. 10684–10695.
- [35] Olaf Ronneberger, Philipp Fischer, and Thomas Brox. 2015. U-net: Convolutional networks for biomedical image segmentation. In *International Conference on Medical Image Computing and Computer Assisted Intervention (MICCAI)*. Springer, 234–241.
- [36] Ludan Ruan, Yiyang Ma, Huan Yang, Huiguo He, Bei Liu, Jianlong Fu, Nicholas Jing Yuan, Qin Jin, and Baining Guo. 2023. Mm-diffusion: Learning multi-modal diffusion models for joint audio and video generation. In *Conference on Computer Vision and Pattern Recognition (CVPR)*. 10219–10228.
- [37] Sakib Shahriar. 2022. GAN computers generate arts? A survey on visual arts, music, and literary text generation using generative adversarial network. *Displays* 73 (2022), 102237.
- [38] Xuyang Shen, Dong Li, Jinxing Zhou, Zhen Qin, Bowen He, Xiaodong Han, Aixuan Li, Yuchao Dai, Lingpeng Kong, Meng Wang, et al. 2023. Fine-grained audible video description. In *Conference on Computer Vision and Pattern Recognition (CVPR)*. 10585–10596.
- [39] Uriel Singer, Adam Polyak, Thomas Hayes, Xi Yin, Jie An, Songyang Zhang, Qiuyan Hu, Harry Yang, Oron Ashual, Oran Gafni, et al. 2022. Make-A-Video: Text-to-Video Generation without Text-Video Data. In *International Conference on Learning Representations (ICLR)*.
- [40] Jascha Sohl-Dickstein, Eric A. Weiss, Niru Maheswaranathan, and Surya Ganguli. 2015. Deep Unsupervised Learning using Nonequilibrium Thermodynamics. In *International Conference on Machine Learning (ICML)*. 2256–2265.
- [41] Jiaming Song, Chenlin Meng, and Stefano Ermon. 2020. Denoising Diffusion Implicit Models. In *International Conference on Learning Representations (ICLR)*.
- [42] Jianlin Su, Murtadha Ahmed, Yu Lu, Shengfeng Pan, Wen Bo, and Yunfeng Liu. 2024. Roformer: Enhanced transformer with rotary position embedding. *Neurocomputing* 568 (2024), 127063.
- [43] Kim Sung-Bin, Arda Senocak, Hyunwoo Ha, Andrew Owens, and Tae-Hyun Oh. 2023. Sound to visual scene generation by audio-to-visual latent alignment. In *Conference on Computer Vision and Pattern Recognition (CVPR)*. 6430–6440.
- [44] Thomas Unterthiner, Sjoerd Van Steenkiste, Karol Kurach, Raphaël Marinier, Marcin Michalski, and Sylvain Gelly. 2018. Towards accurate generative models of video: A new metric & challenges. *arXiv preprint arXiv:1812.01717* (2018).
- [45] Thomas Unterthiner, Sjoerd van Steenkiste, Karol Kurach, Raphaël Marinier, Marcin Michalski, and Sylvain Gelly. 2019. FVD: A new metric for video generation. (2019).
- [46] Ashish Vaswani, Noam Shazeer, Niki Parmar, Jakob Uszkoreit, Llion Jones, Aidan N Gomez, Łukasz Kaiser, and Illia Polosukhin. 2017. Attention is all you need. *Conference on Neural Information Processing Systems (NeurIPS)* 30 (2017).

929
930
931
932
933
934
935
936
937
938
939
940
941
942
943
944
945
946
947
948
949
950
951
952
953
954
955
956
957
958
959
960
961
962
963
964
965
966
967
968
969
970
971
972
973
974
975
976
977
978
979
980
981
982
983
984
985
986987
988
989
990
991
992
993
994
995
996
997
998
999
1000
1001
1002
1003
1004
1005
1006
1007
1008
1009
1010
1011
1012
1013
1014
1015
1016
1017
1018
1019
1020
1021
1022
1023
1024
1025
1026
1027
1028
1029
1030
1031
1032
1033
1034
1035
1036
1037
1038
1039
1040
1041
1042
1043
1044

| | | | |
|------|------|---|------|
| 1045 | [47] | Yaohui Wang, Xinyuan Chen, Xin Ma, Shangchen Zhou, Ziqi Huang, Yi Wang, Ceyuan Yang, Yinan He, Jiashuo Yu, Peiqing Yang, et al. 2023. Lavie: High-quality video generation with cascaded latent diffusion models. <i>arXiv preprint arXiv:2309.15103</i> (2023). | 1103 |
| 1046 | | | 1104 |
| 1047 | | | 1105 |
| 1048 | [48] | Chenfei Wu, Lun Huang, Qianxi Zhang, Binyang Li, Lei Ji, Fan Yang, Guillermo Sapiro, and Nan Duan. 2021. Godiva: Generating open-domain videos from natural descriptions. <i>arXiv preprint arXiv:2104.14806</i> (2021). | 1106 |
| 1049 | | | 1107 |
| 1050 | [49] | Jay Zhangjie Wu, Yixiao Ge, Xintao Wang, Stan Weixian Lei, Yuchao Gu, Yufei Shi, Wynne Hsu, Ying Shan, Xiaohu Qie, and Mike Zheng Shou. 2023. Tune-a-video: One-shot tuning of image diffusion models for text-to-video generation. In <i>International Conference on Computer Vision (ICCV)</i> . 7623–7633. | 1108 |
| 1051 | | | 1109 |
| 1052 | | | 1110 |
| 1053 | [50] | Yazhou Xing, Yingqing He, Zeyue Tian, Xintao Wang, and Qifeng Chen. 2024. Seeing and Hearing: Open-domain Visual-Audio Generation with Diffusion Latent Aligners. <i>arXiv preprint arXiv:2402.17723</i> (2024). | 1111 |
| 1054 | | | 1112 |
| 1055 | [51] | Zhen Xing, Qi Dai, Han Hu, Zuxuan Wu, and Yu-Gang Jiang. 2023. Simda: Simple diffusion adapter for efficient video generation. <i>arXiv preprint arXiv:2308.09710</i> (2023). | 1113 |
| 1056 | | | 1114 |
| 1057 | [52] | Jun Xu, Tao Mei, Ting Yao, and Yong Rui. 2016. Msr-vtt: A large video description dataset for bridging video and language. In <i>Conference on Computer Vision and Pattern Recognition (CVPR)</i> . 5288–5296. | 1115 |
| 1058 | | | 1116 |
| 1059 | [53] | Dongchao Yang, Jianwei Yu, Helin Wang, Wen Wang, Chao Weng, Yuexian Zou, and Dong Yu. 2023. Diffsound: Discrete diffusion model for text-to-sound generation. <i>IEEE/ACM Transactions on Audio, Speech, and Language Processing (IEEE-ACM T AUDIO SPE)</i> (2023). | 1117 |
| 1060 | | | 1118 |
| 1061 | | | 1119 |
| 1062 | | | 1120 |
| 1063 | | | 1121 |
| 1064 | | | 1122 |
| 1065 | | | 1123 |
| 1066 | | | 1124 |
| 1067 | | | 1125 |
| 1068 | | | 1126 |
| 1069 | | | 1127 |
| 1070 | | | 1128 |
| 1071 | | | 1129 |
| 1072 | | | 1130 |
| 1073 | | | 1131 |
| 1074 | | | 1132 |
| 1075 | | | 1133 |
| 1076 | | | 1134 |
| 1077 | | | 1135 |
| 1078 | | | 1136 |
| 1079 | | | 1137 |
| 1080 | | | 1138 |
| 1081 | | | 1139 |
| 1082 | | | 1140 |
| 1083 | | | 1141 |
| 1084 | | | 1142 |
| 1085 | | | 1143 |
| 1086 | | | 1144 |
| 1087 | | | 1145 |
| 1088 | | | 1146 |
| 1089 | | | 1147 |
| 1090 | | | 1148 |
| 1091 | | | 1149 |
| 1092 | | | 1150 |
| 1093 | | | 1151 |
| 1094 | | | 1152 |
| 1095 | | | 1153 |
| 1096 | | | 1154 |
| 1097 | | | 1155 |
| 1098 | | | 1156 |
| 1099 | | | 1157 |
| 1100 | | | 1158 |
| 1101 | | | 1159 |
| 1102 | | | 1160 |
| | | | 1161 |
| | | | 1162 |
| | | | 1163 |
| | | | 1164 |
| | | | 1165 |
| | | | 1166 |
| | | | 1167 |
| | | | 1168 |
| | | | 1169 |
| | | | 1170 |
| | | | 1171 |
| | | | 1172 |
| | | | 1173 |
| | | | 1174 |
| | | | 1175 |
| | | | 1176 |
| | | | 1177 |
| | | | 1178 |
| | | | 1179 |
| | | | 1180 |
| | | | 1181 |
| | | | 1182 |
| | | | 1183 |
| | | | 1184 |
| | | | 1185 |
| | | | 1186 |
| | | | 1187 |
| | | | 1188 |
| | | | 1189 |
| | | | 1190 |
| | | | 1191 |
| | | | 1192 |
| | | | 1193 |
| | | | 1194 |
| | | | 1195 |
| | | | 1196 |
| | | | 1197 |
| | | | 1198 |
| | | | 1199 |
| | | | 1200 |
| | | | 1201 |
| | | | 1202 |
| | | | 1203 |
| | | | 1204 |
| | | | 1205 |
| | | | 1206 |
| | | | 1207 |
| | | | 1208 |
| | | | 1209 |
| | | | 1210 |
| | | | 1211 |
| | | | 1212 |
| | | | 1213 |
| | | | 1214 |
| | | | 1215 |
| | | | 1216 |
| | | | 1217 |
| | | | 1218 |
| | | | 1219 |
| | | | 1220 |
| | | | 1221 |
| | | | 1222 |
| | | | 1223 |
| | | | 1224 |
| | | | 1225 |
| | | | 1226 |
| | | | 1227 |
| | | | 1228 |
| | | | 1229 |
| | | | 1230 |
| | | | 1231 |
| | | | 1232 |
| | | | 1233 |
| | | | 1234 |
| | | | 1235 |
| | | | 1236 |
| | | | 1237 |
| | | | 1238 |
| | | | 1239 |
| | | | 1240 |
| | | | 1241 |
| | | | 1242 |
| | | | 1243 |
| | | | 1244 |
| | | | 1245 |
| | | | 1246 |
| | | | 1247 |
| | | | 1248 |
| | | | 1249 |
| | | | 1250 |
| | | | 1251 |
| | | | 1252 |
| | | | 1253 |
| | | | 1254 |
| | | | 1255 |
| | | | 1256 |
| | | | 1257 |
| | | | 1258 |
| | | | 1259 |
| | | | 1260 |
| | | | 1261 |
| | | | 1262 |
| | | | 1263 |
| | | | 1264 |
| | | | 1265 |
| | | | 1266 |
| | | | 1267 |
| | | | 1268 |
| | | | 1269 |
| | | | 1270 |
| | | | 1271 |
| | | | 1272 |
| | | | 1273 |
| | | | 1274 |
| | | | 1275 |
| | | | 1276 |
| | | | 1277 |
| | | | 1278 |
| | | | 1279 |
| | | | 1280 |
| | | | 1281 |
| | | | 1282 |
| | | | 1283 |
| | | | 1284 |
| | | | 1285 |
| | | | 1286 |
| | | | 1287 |
| | | | 1288 |
| | | | 1289 |
| | | | 1290 |
| | | | 1291 |
| | | | 1292 |
| | | | 1293 |
| | | | 1294 |
| | | | 1295 |
| | | | 1296 |
| | | | 1297 |
| | | | 1298 |
| | | | 1299 |
| | | | 1300 |
| | | | 1301 |
| | | | 1302 |
| | | | 1303 |
| | | | 1304 |
| | | | 1305 |
| | | | 1306 |
| | | | 1307 |
| | | | 1308 |
| | | | 1309 |
| | | | 1310 |
| | | | 1311 |
| | | | 1312 |
| | | | 1313 |
| | | | 1314 |
| | | | 1315 |
| | | | 1316 |
| | | | 1317 |
| | | | 1318 |
| | | | 1319 |
| | | | 1320 |
| | | | 1321 |
| | | | 1322 |
| | | | 1323 |
| | | | 1324 |
| | | | 1325 |
| | | | 1326 |
| | | | 1327 |
| | | | 1328 |
| | | | 1329 |
| | | | 1330 |
| | | | 1331 |
| | | | 1332 |
| | | | 1333 |
| | | | 1334 |
| | | | 1335 |
| | | | 1336 |
| | | | 1337 |
| | | | 1338 |
| | | | 1339 |
| | | | 1340 |
| | | | 1341 |
| | | | 1342 |
| | | | 1343 |
| | | | 1344 |
| | | | 1345 |
| | | | 1346 |
| | | | 1347 |
| | | | 1348 |
| | | | 1349 |
| | | | 1350 |
| | | | 1351 |
| | | | 1352 |
| | | | 1353 |
| | | | 1354 |
| | | | 1355 |
| | | | 1356 |
| | | | 1357 |
| | | | 1358 |
| | | | 1359 |
| | | | 1360 |
| | | | 1361 |
| | | | 1362 |
| | | | 1363 |
| | | | 1364 |
| | | | 1365 |
| | | | 1366 |
| | | | 1367 |
| | | | 1368 |
| | | | 1369 |
| | | | 1370 |
| | | | 1371 |
| | | | 1372 |
| | | | 1373 |
| | | | 1374 |
| | | | 1375 |
| | | | 1376 |
| | | | 1377 |
| | | | 1378 |
| | | | 1379 |
| | | | 1380 |
| | | | 1381 |
| | | | 1382 |
| | | | 1383 |
| | | | 1384 |
| | | | 1385 |
| | | | 1386 |
| | | | 1387 |
| | | | 1388 |
| | | | 1389 |
| | | | 1390 |
| | | | 1391 |
| | | | 1392 |
| | | | 1393 |
| | | | 1394 |
| | | | 1395 |
| | | | 1396 |
| | | | 1397 |
| | | | 1398 |
| | | | 1399 |
| | | | 1400 |
| | | | 1401 |
| | | | 1402 |
| | | | 1403 |
| | | | 1404 |
| | | | 1405 |
| | | | 1406 |
| | | | 1407 |
| | | | 1408 |
| | | | 1409 |
| | | | 1410 |
| | | | 1411 |
| | | | 1412 |
| | | | 1413 |
| | | | 1414 |
| | | | 1415 |
| | | | 1416 |
| | | | 1417 |
| | | | 1418 |
| | | | 1419 |
| | | | 1420 |
| | | | 1421 |
| | | | 1422 |
| | | | 1423 |
| | | | 1424 |
| | | | 1425 |
| | | | 1426 |
| | | | 1427 |
| | | | 1428 |
| | | | 1429 |
| | | | 1430 |
| | | | 1431 |
| | | | 1432 |
| | | | 1433 |
| | | | 1434 |
| | | | 1435 |
| | | | 1436 |
| | | | 1437 |
| | | | 1438 |
| | | | 1439 |
| | | | 1440 |
| | | | 1441 |
| | | | 1442 |
| | | | 1443 |
| | | | 1444 |
| | | | 1445 |
| | | | 1446 |
| | | | 1447 |
| | | | 1448 |
| | | | 1449 |
| | | | 1450 |
| | | | 1451 |
| | | | 1452 |
| | | | 1453 |
| | | | 1454 |
| | | | 1455 |
| | | | 1456 |
| | | | 1457 |
| | | | 1 |